Potential anisotropic finite-time singularity in the three-dimensional axisymmetric Euler equations

Sergio Rica

Instituto de Física, Pontificia Universidad Católica de Chile, Avenida Vicuña Mackenna 4860, Santiago, Chile

(Received 31 January 2021; accepted 7 March 2022; published 31 March 2022)

The search of finite-time singularity solutions of Euler equations is considered for the case of an incompressible and inviscid fluid. Under the assumption that a finite-time blow-up solution may be spatially anisotropic as time goes by such that the flow contracts more rapidly into one direction than into the other, it can be shown that the dynamics of an axially symmetric flow with swirl may be approximated to a simpler hyperbolic system. By using the method of characteristics, it can be shown that generically the velocity flow exhibits multivalued solutions appearing on a rim at a finite distance from the axis of rotation, which displays a singular behavior in the radial derivatives of velocities. Moreover, the general solution shows a genuine blow-up, which is also discussed. This singularity is generic for a vast number of smooth finite-energy initial conditions and is characterized by a local singular behavior of velocity gradients and accelerations.

DOI: 10.1103/PhysRevFluids.7.034401

I. INTRODUCTION

Despite more than 250 years of history, a general understanding of the properties of solutions of Euler equations remains an open problem. In particular, we have the so-called regularity problem or the possible existence of finite-time singularity solutions: Does a smooth initial condition for the velocity field remain regular for all times as the velocity flow evolves in accordance with Euler equations for an inviscid and incompressible fluid? By smooth, we mean that the initial condition is differentiable everywhere and of finite energy [see the definition equation (8) below], which is one of the invariants of the dynamics. Although Euler's (and Navier-Stokes') equations look simple, they are partial differential equations that are hard to solve because they are of nonlinear and nonlocal character, therefore the above-mentioned question remains elusive, as does, for instance, the turbulent motion in the Navier-Stokes equations.

The search for singularities of solutions of Euler equations for fluids in three space dimensions is not new. In fact, the first attempts date back to the early 20th century [1,2]. In the 1930s, Leray [3] suggested the possibility of a self-similar solution of Navier-Stokes equations in which the velocity field scales as a power law in time. Following Leray's endeavor, Pomeau [4–7], Chae [8–10], and others revisited the possible existence of pointlike spatiotemporal singularities. Nevertheless, Leray's explicit self-similar equations for singularities led to a very challenging problem that is far from being fully understood. Unfortunately, this approach has not been successful in providing an explicit example of this type of singularity.

In general, theoretical physics allows for the possible existence of singular behaviors that may be regarded as internal paradoxes. Some examples of singular solutions in partial differential equations are the electric field created by a pointlike charge, the magnetic field induced by a current in a wire, a vortex ring in an incompressible fluid [11,12], and the space-time singularities in general relativity [13], to name a few examples.

In the context of fluid motion, a geometric approach based on singular structures such as vortex sheets successfully manifests a singular behavior [14]. Similarly, Siggia suggested that interactions of vortex filaments may result in this kind of self-similar reconnection [15,16]. However, an asymptotic limit for a solution of Euler equations in singular manifolds is not entirely satisfactory because of the lack of any intrinsic length in the Euler equations.

In the past 40 years, as a consequence of improvements in computer technology, the question of regularity saw renewed interest from a numerical and theoretical standpoint. Both physicists and mathematicians made an enormous effort in the search for possible singular solutions of Euler equations. To mention a few, the Taylor-Green initial condition was considered in Refs. [17–19], antiparallel vortex tubes were considered in Refs. [20–22], and highly symmetric Kida flow was addressed in Ref. [23]. The reader is referred to the article by Gibbon [24], who carefully reviews the most notable progress, including a summary table with expectations of the existence, or not, of finite-time blow-up solutions of Euler equations as well as Navier-Stokes equations. More recently, Luo and Hou [25] provided numerical evidence of the existence of a finite-time blow-up for the axially symmetric Euler equations at the outer boundary of the domain, and Barkley [26] analyzed this singularity from a hydrodynamic aspect, showing that the formation of the singularity is driven by the wall. Lastly, Elgindi and Jeong proved the existence of a finite-time singularity of axially symmetric Euler equations in an "hourglass"-like domain excluding the axis of rotation [27]. The question of the existence of such singularities in the whole space remained as an open problem until 2021, when Elgindi [28] showed how, under certain assumptions, the nonlocal contribution of vorticity can be simplified in the case of an axisymmetric flow without swirl exhibiting a self-similar blow-up in finite time.

In this article, we consider the possibility that due to fluid stretching, the flow could destroy the spatial isotropy, modifying the temporal evolution of the flow, ruled by Euler equations, and spontaneously the dynamics generates a space anisotropy inducing a flow that may shrink more rapidly in one direction than the other. Indeed, this process is supported by the numerical work of Kerr (see Figs. 2 and 4 of Ref. [20]), as well as some recent work by Brenner, Hormoz, and Pumir [29]. Under this assumption, we show that the axisymmetric flow may be approximated by a hyperbolic system, which is solved using the method of characteristic. It is shown that, generically, the radial and swirl velocities become multivalued functions at a rim at a finite distance from the axis of rotation exhibiting a singularity of some velocity derivatives.

The current singularity appears to be different from that found recently by Elgindi [28]. In the current paper, the singularity is a consequence of the advective structure of the flow dynamics together with the swirl and an adequate initial condition for the velocity flow. The advection effect causes the velocity flow to be a multivalued function at some time t_c; in addition, $\frac{\partial v_r}{\partial r} \sim 1/(t_c - t)$. Contrarily, in Ref. [28], as a consequence of a property exhibited by the axisymmetric flow without swirl, the advective term, $\boldsymbol{v} \cdot \boldsymbol{\nabla}$, can be discarded in the vorticity equation [Eq. (5) below], while the nonlocality (a simplified Biot-Savart integral) exhibits a genuine finite-time singularity, similar to the one studied by Constantin, Lax, and Majda [30] and De Gregorio [31,32] in the 1980s and 1990s, respectively.

A better knowledge of the nature of solutions of Euler or Navier-Stokes equations may pave the way from Leray's original idea for approaching the problem of turbulence [5,6]. Indeed, based on the self-focusing nonlinear Schrödinger equation, in collaboration with Josserand and Pomeau, we suggested a singularity-mediated turbulent scenario for the observed intermittency in fully developed turbulence [33].

The paper is organized as follows: Section II introduces Euler equations and their basic properties, namely symmetries and conserved laws. Further, the Leray finite-time singularity approach is briefly reviewed. In Sec. III, the equations for an axially symmetric flow with swirl are introduced. In this situation, a tridimensional velocity field plus pressure is reduced to a coupled system of two partial differential equations. Next, the main assumption of the paper allows us to simplify the axisymmetric flow, making it possible to obtain an explicit solution. Section IV presents the main result of the paper, in which we show, via the method of characteristic, that the simplified

anisotropic model shows two consecutive singularities in time. A primary singularity arises as the radial and swirl velocities become multivalued functions in the Eulerian description. This singularity is formally followed by a later singularity inside the multivalued domain. Section V concludes with a general discussion and future perspectives. Appendix A presents a qualitative point of view by employing tools taken from the Hamiltonian dynamical system theory, and Appendix B presents a particular infinite energy solution exhibiting a finite-time singular behavior in the axisymmetric reduced model.

II. EULER EQUATIONS

Euler equations for an inviscid and incompressible fluid read

$$\frac{\partial}{\partial t}\boldsymbol{v}(\boldsymbol{x},t)+\boldsymbol{v}\cdot\boldsymbol{\nabla}\ \boldsymbol{v}=-\boldsymbol{\nabla}p, \tag{1}$$

$$\boldsymbol{\nabla}\cdot\boldsymbol{v}=\boldsymbol{0}. \tag{2}$$

These equations are complemented by boundary conditions plus the initial flow velocity. For the boundary conditions, as we clarify later on, we assume that the velocity field decreases at infinity such that $\lim_{r\to\infty}|\boldsymbol{v}|^2r^3\to 0$. In addition to Eqs. (1) and (2), one needs a divergence-free initial condition that reads

$$\boldsymbol{v}(\boldsymbol{x},t=0)=\boldsymbol{v}_0(\boldsymbol{x}),$$
$$\boldsymbol{\nabla}\cdot\boldsymbol{v}_0=\boldsymbol{0}. \tag{3}$$

Equivalently, taking the curl of (1) eliminates the pressure term. This procedure gives an equation for the vorticity field:

$$\boldsymbol{\omega}=\boldsymbol{\nabla}\times\boldsymbol{v}. \tag{4}$$

The vorticity (or the Helmholtz) equation reads

$$\partial_t\boldsymbol{\omega}+\boldsymbol{v}\cdot\boldsymbol{\nabla}\boldsymbol{\omega}=\boldsymbol{\omega}\cdot\boldsymbol{\nabla}\boldsymbol{v}. \tag{5}$$

The right-hand side in (5) represents vorticity stretching: everywhere in the space, locally, the vorticity experiences a growth in one direction and a contraction into the other direction.

From a more taxonomic point of view, Euler equations are a set of nonlinear and nonlocal partial differential equations. The nonlocality comes from the pressure term, $p(\boldsymbol{x},t)$, which, after taking the divergence of (1), follows as a solution of a Poisson equation:

$$\boldsymbol{\nabla}^2p=-\partial_{ik}(v_iv_k)\equiv-\partial_iv_k\partial_kv_i. \tag{6}$$

Here repeated indices stand for a sum, as in Einstein's convention. Thus, the pressure contribution becomes a nonlocal functional of the right-hand side of (6). Similarly, the Helmholtz equation (5) is also a nonlinear and nonlocal partial differential equation: the velocity in (5) is a nonlocal functional of vorticity (4) as follows from the Biot-Savart law:

$$\boldsymbol{v}(\boldsymbol{x})=\frac{1}{4\pi}\int\boldsymbol{\omega}(\boldsymbol{x}')\times\frac{(\boldsymbol{x}-\boldsymbol{x}')}{|\boldsymbol{x}-\boldsymbol{x}'|^3}\,d\boldsymbol{x}'. \tag{7}$$

Euler equations, as well as Helmholtz equations, possess a number of symmetries and conserved quantities. Among these are space-time translational symmetry, time reversibility, rotational invariance, Galilean invariance, and scale invariance. The last symmetry tells us the following: if $\forall\,\ell\in\mathbb{R}\,\&\,\tau\in\mathbb{R}$, and if $\boldsymbol{v}(\boldsymbol{x},t)$ and $p(\boldsymbol{x},t)$ are solutions of (1) and (2), then $\frac{\ell}{\tau}\boldsymbol{v}(\boldsymbol{x}/\ell,t/\tau)$ and $\frac{\ell^2}{\tau^2}p(\boldsymbol{x}/\ell,t/\tau)$ are also solutions of (1) and (2). This scale-invariance symmetry is the basis of Leray's self-similar solutions, which are discussed later on.

Some conserved quantities in the Euler equations are the kinetic energy, linear momentum, total vorticity, circulation conservation, and helicity conservation, among others. We refer the reader to relevant textbooks for a deeper and additional review on conserved quantities [11,34,35].

The kinetic energy reads

$$\mathcal{E} = \frac{1}{2}\int_{\mathbb{R}^3} |\boldsymbol{v}(\boldsymbol{x}, t)|^2 \, d\boldsymbol{x}. \tag{8}$$

Then, from (1) and (2), we obtain the conservation of energy (8), i.e.,

$$\frac{d\mathcal{E}}{dt} = 0.$$

In the following, except for Appendix B, we restrict the discussion to finite energy flows, therefore the initial condition must satisfy

$$\int_{\mathbb{R}^3} |\boldsymbol{v}_0(\boldsymbol{x})|^2 \, d\boldsymbol{x} < \infty.$$

It is worth mentioning that infinite energy blow-up solutions could be found in the existing literature [36].

In 1934, Leray [3] suggested a pointlike singularity at the origin solution of equations of fluid dynamics (1) and (2) of the form

$$\boldsymbol{v}(\boldsymbol{x}, t) = \frac{1}{(t_c - t)^{1-\beta}} \boldsymbol{V}\left(\frac{\boldsymbol{x}}{(t_c - t)^{\beta}}\right).$$

Originally, Leray set $\beta = 1/2$ as it was a parameter fixed by viscosity in the Navier-Stokes equations. In that situation, i.e., $\beta = 1/2$, Nečas, Růžička, and Šverák showed that the only solution for $\boldsymbol{V}(\cdot)$ satisfying the Navier-Stokes-Leray equations is $\boldsymbol{V} = \boldsymbol{0}$ [37]. However, the absence of viscosity together with scale-invariance symmetry leaves open any possible relation between length and time, thus, *a priori*, β is not fixed by dimensional analysis. We underline that a given initial value of energy or circulation may set a characteristic length, e.g., $\beta = 2/5$ characterizes a flow in which the initial energy, $\mathcal{E}$, fixes the scales; $\beta = 1/2$ corresponds to a scale fixed by circulation. Different exponents have been considered by Pomeau *et al.* [4–7] and Chae [8–10] in a series of papers. Despite those efforts, a satisfactory solution of the resulting self-similar Euler-Leray equations, satisfying the right boundary conditions, has become a very challenging problem, perhaps harder than the original time-dependent Euler Eqs. (1) and (2).

Until now, the still unknown Leray singularities have been supposed as isotropic. That is, presumably the flow evolves independently of initial fluctuations toward a similar scaling of all coordinates in time, or in other words, all principal axes scale in time with the same rate. Nevertheless, there is no reason to exclude the possibility that the self-similar velocity field may scale in an anisotropic way in time. It is plausible that initial fluctuations may be amplified in one direction more than in another. This process is supported by the numerical work of Refs. [20] and [29]. Indeed, it has been suggested that vorticity stretching [the right-hand side of (5)] deforms vorticity to the extent that an initial elliptic vortex distribution is deformed in such a way that it becomes a vortex sheet as time evolves. Moreover, a simple argument based on a generic feature of the strain tensor, $\partial_k v_i + \partial_i v_k$, indicates the existence of a dynamical "shrink" of at least one coordinate: because of incompressibility, this symmetric tensor is locally traceless at all points in the domain, therefore everywhere at least one eigenvalue must be negative and another must be positive.

By following an idea by Kasner [38] for an anisotropic scaling of the space-time metric in general relativity, the following anisotropic self-similar velocity field is suggested:

$$v_i(\boldsymbol{x}, t) = \frac{1}{(t_c - t)^{1-\beta_i}} V_i\left(\frac{x_1}{(t_c - t)^{\beta_1}}, \frac{x_2}{(t_c - t)^{\beta_2}}, \frac{x_3}{(t_c - t)^{\beta_3}}\right). \tag{9}$$

The advantage of this dependence is that the divergence-free condition (2) is preserved in the self-similar variables, and more importantly, spatial gradients along with different components are weaker than others, allowing a simpler systematic asymptotic analysis as $t \to t_c^-$. Replacing (9) in the Euler equations, one gets that the pressure term $-\nabla p$ becomes relevant just in the direction of the largest β_i. This observation opens the door to a new approach in the search for finite-time singularities of Euler equations, and it is the general approach that will be pursued in a separate publication.

In the following section (Sec. III), the assumption is applied of the anisotropic scaling to the simpler case of an axisymmetric flow. In that situation, the assumption $\beta_1 = \beta_2 < \beta_3$ allows the approximation for the ith component of the velocity,

$$\left|\frac{\partial v_i}{\partial x}\right| \approx \left|\frac{\partial v_i}{\partial y}\right| \ll \left|\frac{\partial v_i}{\partial z}\right|, \tag{10}$$

simplifying the original 3D Euler equations.

III. THE AXISYMMETRIC FLOW WITH SWIRL

In the case of an axisymmetric flow, there is no dependence of any velocity on the angular variable, ϕ, in cylindrical coordinates [12]. The velocity and vorticity fields read, respectively,

$$\boldsymbol{v} = (v_r(r,z,t), v_\phi(r,z,t), v_z(r,z,t)),$$
$$\boldsymbol{\omega} = \left(-\frac{\partial v_\phi}{\partial z}, \frac{\partial v_r}{\partial z} - \frac{\partial v_z}{\partial r}, \frac{1}{r}\frac{\partial (r v_\phi)}{\partial r}\right).$$

The incompressibility condition

$$\nabla \cdot \boldsymbol{v} = \frac{1}{r}\frac{\partial (r v_r)}{\partial r} + \frac{\partial v_z}{\partial z} = 0$$

introduces a stream function, $\psi(r,z)$, defined through the relationships

$$v_r = -\frac{1}{r}\frac{\partial \psi}{\partial z}, \qquad v_z = \frac{1}{r}\frac{\partial \psi}{\partial r}. \tag{11}$$

The axial vorticity component reads, in terms of the stream function,

$$\omega_\phi = \frac{\partial v_r}{\partial z} - \frac{\partial v_z}{\partial r} = -\frac{1}{r}\left(\frac{\partial^2 \psi}{\partial r^2} - \frac{1}{r}\frac{\partial \psi}{\partial r} + \frac{\partial^2 \psi}{\partial z^2}\right). \tag{12}$$

Finally, both the vorticity, ω_ϕ, as well as the axial velocity, v_ϕ, rule the self-contained system of partial differential equations [12]:

$$\left(\frac{\partial}{\partial t} + v_r\frac{\partial}{\partial r} + v_z\frac{\partial}{\partial z}\right)\left(\frac{\omega_\phi}{r}\right) = \frac{1}{r^2}\frac{\partial v_\phi^2}{\partial z}, \tag{13}$$

$$\left(\frac{\partial}{\partial t} + v_r\frac{\partial}{\partial r} + v_z\frac{\partial}{\partial z}\right)(r v_\phi) = 0. \tag{14}$$

Equations (13) and (14) together with (11) and (12) are formally a set of two partial differential equations for the fields $\psi(r,z,t)$ and $v_\phi(r,z,t)$. The previous system was already numerically studied in the early 1990s [39,40], and more recently, but in a finite domain, in Refs. [25–27].

The boundary conditions for the axisymmetric flow with swirl at the axis of rotation, $r = 0$, are such that

$$v_r(r=0,z,t) = 0,$$
$$v_\phi(r=0,z,t) = 0,$$
$$\partial_r v_z(r,z,t)|_{r=0} = 0. \tag{15}$$

Moreover, v_r and v_ϕ are odd functions of the radial variable. The velocity boundary conditions (15) imply that the stream function ψ is an even function in the radial coordinate. Thus [25]

$$\left.\frac{\partial^3\psi}{\partial r^3}\right|_{r=0} = 0, \tag{16}$$

and similarly in all other derivatives of odd order. Lastly, the velocity field decreases as $r \to \infty$ and $z \to \pm\infty$ to ensure a finite energy flow.

A. Anisotropic approximation

As previously mentioned, if the flow evolves in an anisotropic fashion, then the z-derivatives are usually larger than the radial ones. Therefore, the relevant approximation for Eq. (12) becomes

$$\omega_\phi \approx -\frac{1}{r}\frac{\partial^2\psi}{\partial z^2},$$

or, in other terms, $|\frac{\partial v_r}{\partial z}| \gg |\frac{\partial v_z}{\partial r}|$. This approximation allows us to simplify Eqs. (13) and (14).

By replacing the above approximation and Eqs. (11) for v_r, v_z into Eq. (13), one obtains (after some simplification)

$$\frac{\partial}{\partial z}\left(\frac{\partial^2\psi}{\partial t\partial z} - \frac{1}{r}\frac{\partial\psi}{\partial z}\frac{\partial^2\psi}{\partial r\partial z} + \frac{1}{r}\frac{\partial\psi}{\partial r}\frac{\partial^2\psi}{\partial z^2} + \frac{1}{r^2}\left(\frac{\partial\psi}{\partial z}\right)^2 + v_\phi^2\right) = 0,$$

from which the expression inside the large parentheses must be independent of z,

$$\frac{\partial^2\psi}{\partial t\partial z} - \frac{1}{r}\frac{\partial\psi}{\partial z}\frac{\partial^2\psi}{\partial r\partial z} + \frac{1}{r}\frac{\partial\psi}{\partial r}\frac{\partial^2\psi}{\partial z^2} + \frac{1}{r^2}\left(\frac{\partial\psi}{\partial z}\right)^2 + v_\phi^2 = I(r,t).$$

Here $I(r,t)$ is a function that may be solved by considering the asymptotic behavior of $\frac{\partial\psi}{\partial z}$, $\frac{\partial\psi}{\partial r}$, and v_ϕ as $z \to \pm\infty$. In the case of finite energy solutions, we impose that both fields $v_\phi \to 0$ and $\frac{\partial\psi}{\partial z} \to 0$ as $z \to \pm\infty$, therefore the function $I(r,t)$ must be identically zero. Then, by setting $I(r,t) = 0$ and adding the swirl velocity equation (14), one gets the final coupled partial differential equations model:

$$\frac{\partial^2\psi}{\partial t\partial z} - \frac{1}{r}\frac{\partial\psi}{\partial z}\frac{\partial^2\psi}{\partial r\partial z} + \frac{1}{r}\frac{\partial\psi}{\partial r}\frac{\partial^2\psi}{\partial z^2} + \frac{1}{r^2}\left(\frac{\partial\psi}{\partial z}\right)^2 + v_\phi^2 = 0, \tag{17}$$

$$\frac{\partial}{\partial t}(rv_\phi) - \frac{1}{r}\frac{\partial\psi}{\partial z}\frac{\partial}{\partial r}(rv_\phi) + \frac{1}{r}\frac{\partial\psi}{\partial r}\frac{\partial}{\partial z}(rv_\phi) = 0. \tag{18}$$

The axisymmetric approximation makes it possible to perform a first integration of $\omega_\phi \approx -\frac{1}{r}\frac{\partial^2\psi}{\partial z^2}$ leading to the set of local partial differential equations (17) and (18) for ψ and v_ϕ. Nevertheless, it must be emphasized that this model is "less nonlocal" because it provides a direct dynamics for $\frac{\partial\psi}{\partial z}$, however $\frac{\partial\psi}{\partial r}$ is also required in Eq. (17) for a complete specification of the dynamics. It should be remarked that the approximation considered here (10) for the present model (17) and (18) is the opposite of Barkley's work [26].

B. Time-dependent reduced model

By defining the following new variables:

$$q = r^2, \quad qJ = \frac{\partial\psi}{\partial z}, \quad zK = \frac{\partial\psi}{\partial q}, \quad \text{and} \quad v_\phi = \sqrt{q}w, \tag{19}$$

and by introducing this change of variable into Eqs. (17) and (18), one gets the following coupled system of partial differential equations:

$$\frac{\partial J}{\partial t} - 2qJ\frac{\partial J}{\partial q} + 2zK\frac{\partial J}{\partial z} = J^2 - w^2, \tag{20}$$

$$\frac{\partial w}{\partial t} - 2qJ\frac{\partial w}{\partial q} + 2zK\frac{\partial w}{\partial z} = 2Jw, \tag{21}$$

$$\frac{\partial (qJ)}{\partial q} = \frac{\partial (zK)}{\partial z}. \tag{22}$$

Equation (22) follows from the condition

$$\frac{\partial^2 \psi}{\partial r \partial z} = \frac{\partial^2 \psi}{\partial z \partial r},$$

and, more important, it traces back the nonlocal aspect of the original Euler equations already discussed.

Equations (20) and (21) are complemented by the initial conditions

$$J(q, z, t = 0) = J_0(q, z), \quad w(q, z, t = 0) = w_0(q, z). \tag{23}$$

Lastly, the boundary conditions read

$$\begin{aligned} J(q = 0, z, t) = \mathcal{J}_0 < \infty, \qquad & w(q = 0, z, t) = \mathcal{W}_0 < \infty, \\ \lim_{q\to\infty} J(q, z, t) \to 0, \qquad & \lim_{q\to\infty} w(q, z, t) \to 0, \\ \lim_{z\to\pm\infty} J(q, z, t) \to 0, \qquad & \lim_{z\to\pm\infty} w(q, z, t) \to 0, \end{aligned} \tag{24}$$

and they must be consistent with a finite-energy solution.

It should be remarked that the question of the existence of a solution exhibiting a finite-time singularity does not depend on the knowledge of $K(q, z, t)$. The vertical velocity and the field $K(q, z, t)$ are both estimated later in Sec. IV E.

IV. SINGULARITY BEHAVIOR IN THE AXISYMMETRIC SIMPLIFIED MODEL

A. Solution of Eqs. (20) and (21) by Riemann's characteristic method

It can be noticed that the set of partial differential equations (20) and (21) together with the initial conditions (23) are written in an Eulerian fashion in which the coordinates (q, z) are fixed in time. In the following, the hyperbolic system (20) and (21) is solved by the method of characteristics. Basically, it consists of passing from an Eulerian description to a Lagrangian one, which reduces (20) and (21) into a system of four ordinary differential equations (ODEs):

$$\frac{dq}{dt} = -2qJ, \tag{25}$$

$$\frac{dz}{dt} = 2zK, \tag{26}$$

$$\frac{dJ}{dt} = J^2 - w^2, \tag{27}$$

$$\frac{dw}{dt} = 2Jw. \tag{28}$$

This ODE system is complemented by the continuous set of initial conditions:

$$q(q_0, z_0, t = 0) = q_0, \tag{29}$$

$$z(q_0, z_0, t = 0) = z_0, \tag{30}$$

$$J(q_0, z_0, t = 0) = J_0(q_0, z_0), \tag{31}$$

$$w(q_0, z_0, t = 0) = w_0(q_0, z_0). \tag{32}$$

The initial conditions (29) and (30) are such that the original Eulerian initial condition (23) is perfectly parametrized by (q_0, z_0).

As already mentioned, condition (22) is only required for the integration of $z(t)$ by using Eq. (26). Otherwise, Eqs. (25), (27), and (28) are independent of (26). In this sense, the variable $z(t)$ just follows, in neither an easy nor a direct way, the dynamics of other variables $q(t)$, $J(t)$, and $w(t)$.

B. The Eulerian-Lagrangian passage of the boundary conditions

The boundary conditions for the original problem (24) must be consistent with the Lagrangian solution by the use of the dynamical system (25)–(28). In particular, the boundary conditions at the axis of rotation are such that both velocities $v_r = v_\phi = 0$ at $r = 0$. The above implies

$$\begin{aligned} \lim_{r\to 0} v_r &= -\lim_{q\to 0} \sqrt{q}\, J(q, z, t) = 0, \\ \lim_{r\to 0} v_\phi &= \lim_{q\to 0} \sqrt{q}\, w(q, z, t) = 0. \end{aligned} \tag{33}$$

Therefore, it is assumed that both $J(0, z_0, t)$ and $w(0, z_0, t)$, remain bounded, a result shown in the following section. Therefore, the boundary conditions (33) at the axis of rotation are fully satisfied. Indeed, the axis is characterized by an initial condition for the dynamical system (25)–(28), i.e., $q_0 = 0$ for $z_0 \in (-\infty, \infty)$. Finally, the axis is well characterized by

$$q(0, z_0, t = 0) = 0, \tag{34}$$

$$z(0, z_0, t = 0) = z_0, \tag{35}$$

$$J(0, z_0, t = 0) = J_0(0, z_0) < \infty, \tag{36}$$

$$w(0, z_0, t = 0) = w_0(0, z_0) < \infty. \tag{37}$$

More importantly, the evolution, as given by Eq. (25), preserves the axis, $q = 0$, since

$$q(0, z_0, t) = 0, \quad \forall\, t \geqslant 0, \quad \text{and} \quad -\infty < z_0 < \infty. \tag{38}$$

In the terminology of the theory of dynamical systems, the axis $r = 0$ ($q = 0$) is called a fixed point of system (25), (27), and (28) (see Appendix A).

C. Exact solution of the dynamical system (25), (27), and (28)

Equations (27) and (28) can be directly integrated by setting $Z = J + iw$, which leads to

$$\frac{dZ}{dt} = Z^2,$$

whose general solution is

$$Z(q_0, z_0, t) = \frac{1}{C(q_0, z_0) - t}, \tag{39}$$

and where $C(q_0, z_0)$ is a complex number related to the initial condition by

$$C(q_0, z_0) = \frac{1}{J_0(q_0, z_0) + i w_0(q_0, z_0)}.$$

In what follows, in order to simplify the notation, we set $C(q_0, z_0) \equiv \tau(q_0, z_0) - i\Delta(q_0, z_0)$, an expression that contains all the required information regarding the initial condition. By splitting into real and imaginary parts in (39), one gets

$$J(q_0, z_0, t) = \frac{\tau(q_0, z_0) - t}{[\tau(q_0, z_0) - t]^2 + \Delta(q_0, z_0)^2}, \tag{40}$$

$$w(q_0, z_0, t) = \frac{\Delta(q_0, z_0)}{[\tau(q_0, z_0) - t]^2 + \Delta(q_0, z_0)^2}. \tag{41}$$

Next, we proceed by integrating (25), obtaining

$$\begin{aligned} q(q_0, z_0, t) &= q(q_0, z_0, 0) e^{-2\int_0^t J(t')dt'} \\ &= q_0 \frac{[\tau(q_0, z_0) - t]^2 + \Delta(q_0, z_0)^2}{\tau(q_0, z_0)^2 + \Delta(q_0, z_0)^2}. \end{aligned} \tag{42}$$

In what follows, we explore the consequences in the behavior of the exact solutions as given by Eqs. (40), (41), and (42).

D. On the appearance of a multivalued velocity flow

The solution of the dynamical system (25)–(28) provides well-defined expressions for $J(q_0, z_0, t)$, $w(q_0, z_0, t)$, and $q(q_0, z_0, t)$ as functions of parameters q_0 and z_0 [Eqs. (34) and (35)] and of the time t. However, the mapping from the Lagrangian to an Eulerian description allows us to show that $J(q, z, t)$ and $w(q, z, t)$ may not necessarily be a single-valued function of q predicting a Riemann-like singularity at some time $t_c > 0$.

Usually, this kind of mechanism is generic and requires only that the coordinate $q(q_0, z_0, t)$, given by (42), becomes a saddle in a point $(q_0^{(c)}, z_0^{(c)})$ at some time t_c. Qualitatively, following Eq. (42), initially ($t = 0$) the coordinate $q(q_0, z_0, t)$ represents an inclined plane with unit slope along the q_0 direction. However, as time goes by this plane becomes deformed, enabling the appearance of a saddle point.

The conditions for the existence of such a saddle read

$$\left.\frac{\partial q}{\partial q_0}\right|_{q_0^{(c)}, z_0^{(c)}, t_c} = 0, \quad \left.\frac{\partial q}{\partial z_0}\right|_{q_0^{(c)}, z_0^{(c)}, t_c} = 0 \quad \text{and} \quad \left.\begin{vmatrix} \frac{\partial^2 q}{\partial q_0^2} & \frac{\partial^2 q}{\partial q_0 \partial z_0} \\ \frac{\partial^2 q}{\partial z_0 \partial q_0} & \frac{\partial^2 q}{\partial z_0^2} \end{vmatrix}\right|_{q_0^{(c)}, z_0^{(c)}, t_c} = 0. \tag{43}$$

The saddle condition (43) determines a critical time t_c for which the multivalued behavior manifests for the first time, as well as its location, $(q_0^{(c)}, z_0^{(c)})$, in terms of the initial conditions. In the Eulerian description, the parametric representation of $J(t)$ versus $q(t)$ shows a singular behavior for $t = t_c$ at a circular rim of finite radius $r_c = \sqrt{q_c}$. Through, Eqs. (40) and (41), it is noticed that both $J(t_c)$ and $w(t_c)$ are finite but their derivatives $\partial J/\partial q$ or $\partial w/\partial q$ diverge. For $t \gtrsim t_c$, the functions $J(t)$ and $w(t)$ become multivalued functions of q in a region near $q \approx q_c$.

To illustrate this transition in a simpler way, let us consider the saddle on the q_0-direction such that the saddle condition (43) arises at $q_0^{(c)}$ finite and $z_0^{(c)} = 0$ (because of translational invariance along the z axis, it is possible to set $z_0^{(c)} = 0$). From the catastrophe theory, it can be seen that near the transition point the coordinate q behaves locally ($q_0 \approx q_0^{(c)}$) as

$$q(q_0, z_0, t) \approx q_c + A(t_c - t)\left(q_0 - q_0^{(c)}\right) + \frac{1}{3}B\left(q_0 - q_0^{(c)}\right)^3 + \frac{1}{2}C z_0^2 + \cdots, \tag{44}$$

where A, B, and C are constants and $q_c = q(q_0^{(c)}, t_c)$ is the value of q at the critical point imposed by the condition (43).

After (44), the basic scaling suggests

$$q - q_c \sim (t_c - t)^{3/2}, \quad q_0 - q_0^{(c)} \sim (t_c - t)^{1/2}, \quad \text{and} \quad z_0 \sim (t_c - t)^{3/4}. \tag{45}$$

Notice that from these scaling laws, the scaling of the z coordinate cannot be accessed. However, the scaling for the flow velocities, $v_r(r, z, t)$ and $v_\phi(r, z, t)$, follows from the formulas

$$v_r = -rJ = -\sqrt{q(q_0, z_0, t)}J(q_0, z_0, t), \tag{46}$$

$$v_\phi = rw = \sqrt{q(q_0, z_0, t)}w(q_0, z_0, t). \tag{47}$$

At the singularity point, $t = t_c$ and $q = q_c$, the values of $J(t_c)$ and $w(t_c)$ are finite, thus both $v_r(t_c)$ and $v_\phi(t_c)$ are also finite. However, their radial derivatives becomes singular. Indeed, the singular behavior comes from expression (44), which leads to

$$\frac{\partial v_r}{\partial r} = 2\sqrt{q}\frac{\partial v_r}{\partial q} = -J(q) - 2q\frac{\partial J}{\partial q}. \tag{48}$$

Because the singularity arises on a rim at finite $q \approx q_c$ and $J(q_c)$ is also finite, it means that the first term in the previous equation is finite. By writing the second term as

$$\frac{\partial J}{\partial q} = \left(\frac{\partial J}{\partial q_0^{(c)}}\right) \Big/ \left(\frac{\partial q}{\partial q_0^{(c)}}\right),$$

one notices that after (44) or (45) the denominator vanishes as $(t_c - t)$, while the numerator is regular. Therefore, the radial velocity gradient on the local plane on which the swirl velocity v_φ vanishes scales as

$$\frac{\partial v_r}{\partial r} \approx -\frac{\gamma}{(t_c - t)}, \tag{49}$$

where the constant

$$\gamma = \frac{2q_c}{A}\frac{\partial J}{\partial q_0}\bigg|_{q_0^c} \tag{50}$$

depends on the parameters at the critical point, and more importantly, it depends on the initial conditions of the flow through $J_0(q_0, z_0)$ and $w_0(q_0, z_0)$. Consequently, by the condition of incompressibility, one also expects $\frac{\partial v_z}{\partial z} \sim \frac{1}{(t_c - t)}$. Although other components of the full stretching tensor, such as $\partial_r v_z$, $\partial_z v_r$, and the vorticity components cannot be determined without the explicit knowledge of z or v_z, the energy dissipation rate

$$\partial_k v_i \partial_k v_i = \frac{v_r^2 + v_\varphi^2}{r^2} + \left(\frac{\partial v_r}{\partial r}\right)^2 + \left(\frac{\partial v_r}{\partial z}\right)^2 + \left(\frac{\partial v_\varphi}{\partial r}\right)^2 + \left(\frac{\partial v_\varphi}{\partial z}\right)^2 + \left(\frac{\partial v_z}{\partial r}\right)^2 + \left(\frac{\partial v_z}{\partial z}\right)^2 \tag{51}$$

diverges at least as $1/(t_c - t)^2$.

Summarizing, in this section it is shown that the general evolution of the velocity field gives rise to a Riemann-like mechanism for which $\frac{\partial v_r}{\partial r}$, as well as $\frac{\partial v_\phi}{\partial r}$, both diverge at a circular rim. The velocity gradient may also diverge, as discussed at the end of the paper. Moreover, in the case of zero swirl velocity, $v_\phi = 0$, a singularity is also expected, but only $\frac{\partial v_r}{\partial r}$ and $\frac{\partial v_z}{\partial z}$ diverge in finite time, while other velocity gradients or vorticity components remain bounded (see Sec. IV H).

Finally, one should notice that, as occurs for compressible fluids, this transition from a single to a multivalued flow could possibly be regularized by viscosity. We shall investigate this issue in a future publication.

E. Vertical velocity field

Up to this stage, through Eqs. (25)–(28), the variables $J(q_0, z_0, t)$, $w(q_0, z_0, t)$, and $q(q_0, z_0, t)$ were solved explicitly, however the function $z(q_0, z_0, t)$ requires knowledge of $K(q_0, z_0, t)$, which hides the nonlocal structure of the incomprehensible Euler equations. However, the velocity field may be estimated by making use of the magnetostatic analogy ($\nabla \cdot \boldsymbol{v} = \boldsymbol{0}$ and $\nabla \times \boldsymbol{v} = \boldsymbol{\omega}$) through the Biot-Savart law (7) for an axisymmetric configuration (this calculation is inspired by a note on Elgindi's approximation by Tao [41]):

$$\psi(r,z,t) = \frac{r}{4\pi}\int \frac{\cos\phi'}{[r'^2 + r^2 - 2r'r\cos\phi' + (z-z')^2]^{1/2}}\,\omega_\phi(r',z',t')\,r'dr'd\phi'dz'.$$

Assuming $\omega_\phi(r',z',t) = -r'\frac{\partial J}{\partial z'}$ for consistency, and after an integration by parts that requires a decaying dependence of $J(r',z',t)$ as $z' \to \pm\infty$, we obtain

$$\psi(r,z,t) = \frac{1}{4\pi}\int \frac{(z-z')rr'\cos\phi'}{[r'^2 + r^2 - 2r'r\cos\phi' + (z-z')^2]^{3/2}}J(r',z',t)\,r'dr'd\phi'dz'.$$

Computing the vertical velocity via (11) gives the following expression for the vertical velocity:

$$\begin{aligned} v_z = &\frac{1}{4\pi r}\int \frac{(z-z')r'\cos\phi'\,J(r',z',t)}{[r'^2 + r^2 - 2r'r\cos\phi' + (z-z')^2]^{3/2}}\,r'dr'd\phi'dz' \\ &- \frac{3}{4\pi}\int \frac{(z-z')r'\cos\phi'(r - r'\cos\phi')\,J(r',z',t)}{[r'^2 + r^2 - 2r'r\cos\phi' + (z-z')^2]^{5/2}}\,r'dr'd\phi'dz'. \end{aligned} \tag{52}$$

It is noticed that because $|J(r',z',t)|$ is bounded, then for the inner behavior, i.e., for $r' < r$ and $|z'| < |z|$, the vertical velocity (and the radial velocity) scales as a length. This property, which is known from magnetostatics (the magnetic field generated by a uniform current is linear in the distance), was used by Elgindi to approximate the Biot-Savart integral. In short, the integrals in (52) are approximated taking $r' \gg r$ via a multipolar expansion. After a direct calculation, we obtain

$$v_z \approx \frac{3}{2}\int_{r'>r}\left(\int_{|z'|>|z|}(z-z')J(r',z',t)dz'\right)\frac{dr'}{r'^2}. \tag{53}$$

Similarly, the leading order for the radial velocity gives

$$v_r \approx -\frac{3r}{4}\int_{r'>r}\left(\int_{|z'|>|z|}J(r',z',t)dz'\right)\frac{dr'}{r'^2}. \tag{54}$$

In particular, in the special case of an odd symmetry (see Sec. IV F), the field $J(r',z',t)$ is an even function with respect to the plane $z' = 0$, and then the integration of $\int_{|z'|>|z|} z'J(r',z',t)dz'$ vanishes in (53). By comparing both expressions (53) and (54) up to leading order in r, it is found that

$$v_z \approx -2z\frac{\partial v_r}{\partial r} \approx \frac{2\gamma z}{(t_c - t)}.$$

Therefore, the function K must scale also as $K \sim \frac{1}{(t_c-t)}$, from which we obtain

$$\frac{dz}{dt} = 2Kz = -\frac{\beta_3}{(t_c - t)}z,$$

thus

$$z(t) \sim (t_c - t)^{\beta_3}.$$

The parameter $\beta_3 = -2\gamma$ does not seem to be universal in the sense of phase transitions or catastrophe theory, but it depends explicitly on the parameter γ defined in (49) and also on the more accurate value of the integrals (54) and (53).

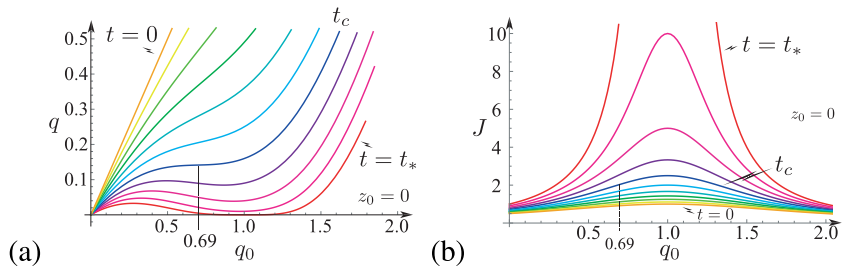

FIG. 1. (a) Plot of the radial coordinate q vs q_0. The saddle condition (43) is sketched in the plot. The critical saddle transition appears for $q_0^c \approx 0.69$ and for a time $t_c \approx 0.61$. (b) Plot of the function $J(q_0)$ (57) as a function of q_0. The plots are done using the initial flow represented by (55) and (56), with the parameters $t_* = q_* = a = b = 1$. In the above figures, the curves are plotted at $z_0 = 0$ and for times spanning into in $0 \leqslant t \leqslant t_*$.

The main lesson of this section is that the hypothesis of an anisotropic exponent is plausible, and the value and sign of β_3 depend essentially on the initial value for the velocity field.

F. Qualitative singular flow

Let us address a situation in which one considers an antisymmetric initial flow [25,26]. This flow is invariant under $z \to -z$ ($z_0 \to -z_0$), $v_\phi \to -v_\phi$, $v_z \to -v_z$, and $v_r \to v_r$. The flow corresponds to an initial condition that causes the swirl velocity to vanish in the line $z_0 = 0$, $\forall\ q_0 \geqslant 0$. A simple choice would be $\Delta(q_0, 0) = 0$ and $\tau(q_0, 0) = \tau_0(q_0)$, where $\tau_0(q_0)$ is a function that has a minimum at q_0^* and $\tau(q_0^*) = t_* > 0$. The advantage in choosing this kind of up-down symmetric flow is that the velocity flow is exactly computed on the plane $z = 0$. The velocity components are $v_r = -\sqrt{q}\, J(q, z = 0, t)$, $v_\phi = 0$, and $v_z = 0$ at $z = 0$. Therefore, the scaling (49) becomes exact at the plane of symmetry $z = 0$.

To illustrate the multivalued behavior, the initial condition can be modeled by setting

$$\tau(q_0, z_0) = \tau_0(q_0) = t_* + a(q_0 - q_*)^2, \tag{55}$$

$$\Delta(q_0, z_0) = b z_0. \tag{56}$$

Although the above initial condition exhibits an infinite energy flow, the ansatz (55) and (56) characterizes the relevant features that the initial flow must possess, that is, $\Delta(q_0, z_0)$ vanishes and $\tau(q_0, z_0)$ has a minimum both in the same line.

In the current case, on the plane $z = 0$, the solutions for J and q read (w vanishes exactly)

$$J(t) = \frac{1}{\tau_0(q_0) - t}, \tag{57}$$

$$q(t) = q_0 \left(1 - \frac{t}{\tau_0(q_0)}\right)^2. \tag{58}$$

Therefore, after Eq. (42) one notices that as t increases, the function $q(q_0, z_0, t)$ changes its monotonicity: it switches from a monotonic increasing function for $t < t_c$ to a nonmonotonic function with at least one maximum and a minimum for $t > t_c$. Figure 1(a) shows the change of concavity in the radial coordinate q versus q_0. Additionally, Fig. 1(b) shows the regular behavior of the function $J(q_0, t)$ at the critical point.

In that situation, one notices that a given q may arise from three different values of q_0, thus $J(q)$ takes three different values. In this way, the function J becomes multivalued, and this transition from a single-valued to a multivalued function represents a singularity.

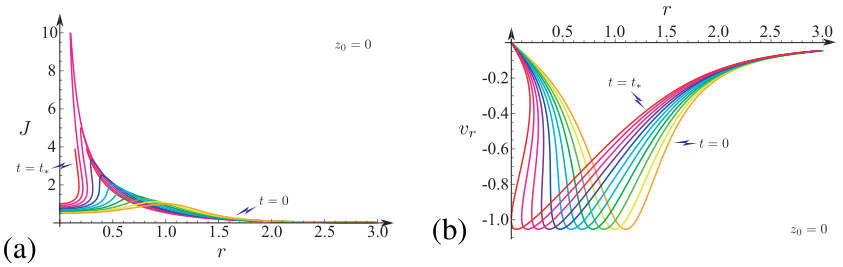

FIG. 2. (a) Parametric plot (with q_0 as the parametrization) of the $J(q_0)$ (57) as a function of the distance from the axis of rotation $r(q_0)$ (58). (b) Parametric plot of the function $v_r(q_0)$ as a function of the distance from the axis of rotation $r(q_0)$. The plots are done using the same representation as in Fig. 1. The swirl velocity is zero for a given initial condition such that $\Delta = 0$.

Figure 2(a) displays parametrically the function, J, as function of the radial distance, r, and, Fig. 2(b) shows the radial velocity, v_r, versus r. Both plots show curves for various times such that $t \leqslant t_*$. One notices that initially both J and v_r in Figs. 2(a) and 2(b) are single-valued functions, but they become multivalued as soon as $t > t_c$.

In the following, we focus on the qualitative behavior of the flow velocities: $v_r(r, z, t)$ and $v_\phi(r, z, t)$ as given by (46) and (47) for the fluid velocity off the $z_0 = 0$ plane. Figure 3 shows J, v_r, and v_ϕ as a function of r for different times as well as different initial planes $z_0 = 1/4$ and $1/2$. One notices that all quantities remain multivalued in the neighborhood of $z_0 = 0$, however these may become single-valued as z_0 increases.

As was already shown, both v_r (46) and v_ϕ (47) vanish at the axis of rotation, $r = 0$. Moreover, one notices the existence of a shear structure of the flow defined by the plane in which $\Delta(q_0, z_0)$ vanishes. For points such that initially $\Delta(q_0, z_0) \approx 0$, the radial and the swirl velocity read

$$v_r \approx -\frac{(t_* - t)}{\sqrt{(t_* - t)^2 + \Delta(q_0, z_0)^2}},$$

$$v_\phi \approx \frac{\Delta(q_0, z_0)}{\sqrt{(t_* - t)^2 + \Delta(q_0, z_0)^2}}.$$

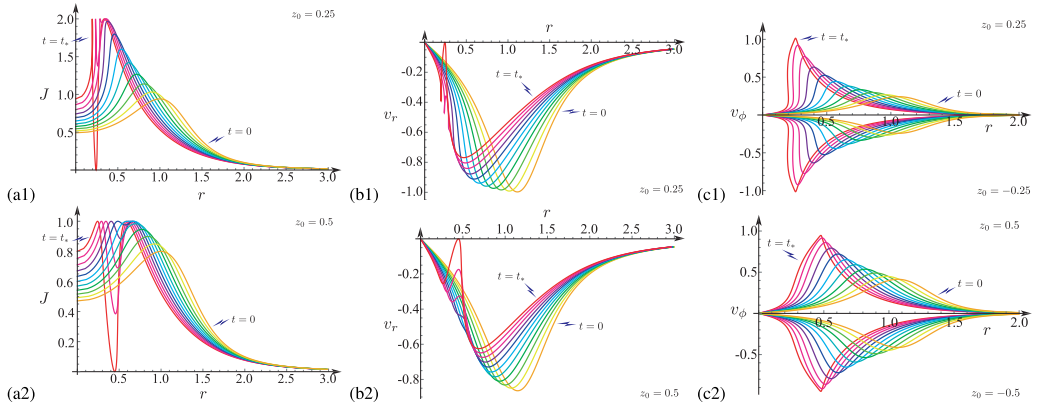

FIG. 3. Parametric plot of the functions: (a1),(a2) J; (b1),(b2) v_r; and, (c1),(c2) v_ϕ vs the distance from the axis of rotation r, for different times varying between $t = 0$ to $t = t_*$. The plots are done using the same parameters as in Fig. 1. The top row 1 corresponds to $z_0 = 1/4$, while the second row corresponds to $z_0 = 1/2$. For the case $z_0 = 1/2$, the quantities J, v_r, and v_ϕ are single-valued functions for all values of r.

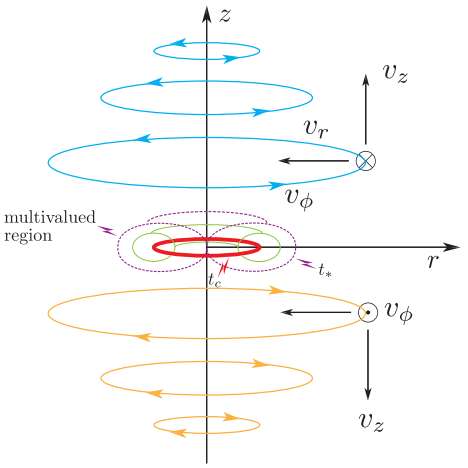

FIG. 4. Qualitative sketch of the singular flow. The radial velocity, v_r, is directed into the axis; the vertical velocity, v_z, shows an outflow coming from the $z = 0$ plane; and the azimuthal velocity, v_ϕ, is drawn into the plane by the symbol $\otimes$ for $z > 0$ and out of the plane by the symbol $\odot$ for $z < 0$ showing a tangential discontinuity. The curves represent the qualitative behavior of streamlines attained by the swirl flow. The swirl velocity v_ϕ is directed downward from the plane for $z > 0$ and in the opposite upward direction for $z < 0$. The radial velocity, v_r, is directed toward the axis of symmetry. Because of the condition $\nabla \cdot \boldsymbol{v} = \mathbf{0}$, the vertical velocity, v_z, must be as shown in the figure. The superposition of the three motions is schematized with streamlines of the swirl flow. The segmented region highlights a spatial zone in which the velocity flow is multivalued.

The radial velocity contracts the flow into the axis, while the swirl flow v_ϕ changes its sign as one crosses the line $\Delta(q_0, z_0) = 0$. Lastly, as a result of the divergence-free flow condition, the v_z component of velocity repels the flow out of the plane defined by $\Delta(q_0, z_0) = 0$. Therefore, the flow suffers a tangential discontinuity. A qualitative sketch of the flow is shown in Fig. 4 and is based on the exact solutions (40) and (41) by using the expressions for the initial velocities described by (55) and (56).

The most striking feature of the flow is that at a time t_c, the radial velocity gradient $\frac{\partial v_r}{\partial r}$ becomes singular located on the plane $z = 0$ at a rim at a finite distance $r_c = \sqrt{q_c}$. Similarly, $\frac{\partial v_\phi}{\partial r}$ becomes singular in the vicinity of the symmetry plane $z = 0$. For $t \gtrsim t_c$, this singular rim grows into a toroidal volume inside which the velocities are multivalued. As $t \to t_*$, the inner side of the toroidal region reaches the axis of rotation, as sketched in Fig. 4.

G. On the existence of a finite-time singularity of $J(t)$

In this section, we show how the formal solution (40), (41), and (42) exhibits a divergence in finite time. Nevertheless, this divergence arises after the formation of multivalued solutions at t_c. Although it appears to be a pure formal singularity, the natural continuation of the solution of (29) and (30) into the multivalued domain still presents some interest because it may play a role whenever multivalued solutions may be regularized by viscosity. Moreover, this kind of singularity resembles the one found by Elgindi [28], and the mathematics has a similarity to the ones that can be found in the works of Constantin, Lax, and Majda [30], and De Gregorio [31,32]. However, the physical mechanisms seem to be different.

Next, we prove the following statement: Let (q_0^*, z_0^*) be a point such that $\Delta(q_0^*, z_0^*) = 0$, and $\tau(q_0^*, z_0^*)$ is the absolute minimum in the manifold $\Delta(q_0^*, z_0^*) = 0$; then $J(q, z, t)$ diverges at time $t_* = \tau(q_0^*, z_0^*) > 0$. This singularity is shown in Fig. 1(b) for $t = t_*$.

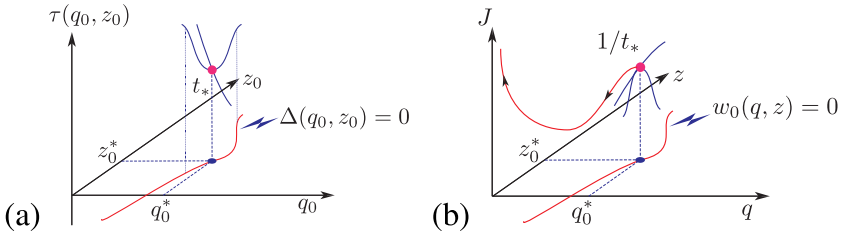

FIG. 5. (a) A generic initial condition for the ODE system (25)–(28). The parameter $\Delta(q_0, z_0)$ vanishes on the curve, and the function $\tau(q_0, z_0)$ reaches a minimum along the curve at $t_* = \tau(q_0^*, z_0^*)$. (b) Sketch of the flow of the dynamical system (25)–(28). Initially, (q, z) matches perfectly with (q_0, z_0), and $J(q_0^*, z_0^*) \equiv 1/t_*$. Then the evolution of $J(t)$, $q(t)$, $z(t)$ drifts away from the original point $(1/t_*, q_0^*, z_0^*)$ to the origin $q = 0$ and $z = 0$ (notice that because of translational invariance in z, we settled the singularity at $z = 0$). Furthermore, at the origin, $J \to \infty$.

The proof of this statement is as follows. Consider an initial point $(\bar{q}_0, \bar{z}_0)$ such that $\Delta(\bar{q}_0, \bar{z}_0) = 0$. Then the denominator in (39) is a pure real number, therefore $Z(\bar{q}_0, \bar{z}_0, t)$ is real and diverges as

$$Z(\bar{q}_0, \bar{z}_0, t) = \frac{1}{[\tau(\bar{q}_0, \bar{z}_0) - t]}$$

when $t \to \tau(\bar{q}_0, \bar{z}_0)$. This singular behavior occurs for all points $(\bar{q}_0, \bar{z}_0)$ on the curve given by the implicit relation $\Delta(\bar{q}_0, \bar{z}_0) = 0$. However, the singularity arises first for the minimal value of all possible $\tau(\bar{q}_0, \bar{z}_0)$, i.e.,

$$t_* = \min_{\bar{q}_0, \bar{z}_0} \{\tau(\bar{q}_0, \bar{z}_0) \,|\, \Delta(\bar{q}_0, \bar{z}_0) = 0\} > 0,$$

from which we obtain $Z(q_0^*, z_0^*, t) = 1/(t_* - t)$ as $t \to t_*$ [see Fig. 5(a)].

In conclusion, it should be remarked that this later or secondary singularity arises as the radial velocity touches the axis of rotation $r = 0$, as seen in Fig. 2(b), thus at t_* the multivalued region reaches the axis of rotation, as shown in Fig. 2(b) for the curve corresponding to $t = t_*$.

H. The case of zero swirl velocity

The multivalued nature of solutions of Eqs. (25), (27), and (28) appears to be generic and independent of the swirl velocity. Therefore, the singular behavior remains in the case of zero swirl velocity; however, in the case of zero swirl velocity, the axial vorticity, driven by Eq. (13), is materially conserved so that

$$\frac{d}{dt}\left(\frac{\omega_\phi}{r}\right) = \frac{d}{dt}\left(-\frac{\partial J}{\partial z}\right) = 0.$$

Moreover, in the case of zero swirl velocity, other components of vorticity vanish, i.e., $\omega_r = \omega_z = 0$.

As has been shown by Ukhovskii-Yudovich [42], if the initial vorticity is sufficiently smooth (class C^∞), then the axially symmetric flow without swirl is globally regular, excluding any singular behavior of the vorticity in finite time. However, if the initial condition is differentiable but not sufficiently smooth, then the global regularity is not known. Recently, Elgindi [28] has shown that an axisymmetric flow without swirl may exhibit a self-similar blow-up in finite time if the initial condition is sufficiently smooth $C^{1,\alpha}$, which is not excluded by the Ukhovskii-Yudovich theorem.

The existence of a multivalued solution exhibiting a singularity of $\frac{\partial v_r}{\partial r}$ and $\frac{\partial v_z}{\partial z}$ may indicate that, despite the fact that initially $J(q, z, t = 0)$ is C^∞, higher derivatives of $\frac{\partial J}{\partial z}$ may not exist as time evolves. This aspect must be regarded carefully in the future.

V. DISCUSSION AND PERSPECTIVES

Under the assumption that Euler (and Helmholtz) equations generate a spatial anisotropy in time, it is shown that the axisymmetric flow with swirl may be approximated by a hyperbolic nonlinear system [Eqs. (17) and (18)], which is solved using the method of characteristics. It is shown that generically, solutions of the approximate system of equations become multivalued in finite time. Under these special conditions as time reaches a critical time t_c, the radial velocity v_r and the swirl velocity v_ϕ remain finite, but the radial derivatives diverge as

$$\frac{\partial v_r}{\partial r} \sim \frac{1}{(t_c - t)} \quad \text{and} \quad \frac{\partial v_\phi}{\partial r} \sim \frac{1}{(t_c - t)}.$$

A second result is that, if initially the axial speed v_ϕ vanishes on a line in the (r, z) plane, then the solution of the approximate model will develop a secondary singularity at some later time $t_* > t_c$.

The complete velocity flow cannot be computed exactly, but it is estimated via the Biot-Savart integral validating a possible hypothesis of the existence of an anisotropic flow.

Lastly, under the assumption of an initial flow with an up-down symmetry, the qualitative velocity flow near the singularity time involves a counter-rotative swirl flow that may be decomposed into an inflow to the central axis, together with a counter rotative axial flow and an outflow from the plane defined by $z = 0$. See the scheme in Fig. 4. In that scenario, and assuming that the flow shrinks into the $z = 0$ plane according $z \sim (t_c - t)^{\beta_3}$ (here β_3 is unknown) and the radial coordinate shrinks into a rim of finite radius r_c as $r - r_c \sim (t_c - t)^{3/2}$ with $\beta_3 > 3/2$ [see (45)], then in accordance with the observed scaling behaviors, one may try a Leray-type approach for Eqs. (17) and (18), which is written as

$$\psi = (t_c - t)^{\beta_3} \Psi\left(\frac{r - r_c}{(t_c - t)^{3/2}}, \frac{z}{(t_c - t)^{\beta_3}}\right),$$

with $\beta_3 > 3/2$, and

$$v_\phi = zW\left(\frac{r - r_c}{(t_c - t)^{3/2}}, \frac{z}{(t_c - t)^{\beta_3}}\right).$$

Here, the prefactor z must be included by the odd symmetry of the flow. According to this basic scaling, one has

$$\begin{aligned} &\psi \sim v_\phi \sim (t_c - t)^{\beta_3}, \quad v_r \sim 1, \quad v_z \sim (t_c - t)^{\beta_3 - 3/2}, \quad \omega_r \sim 1, \\ &\omega_\phi \sim \frac{1}{(t_c - t)^{\beta_3}}, \quad \text{and} \quad \omega_z \sim \frac{1}{(t_c - t)^{3/2}}. \end{aligned} \tag{59}$$

Thus, $v_z \sim (t_c - t)^{\beta_3 - 3/2}$, so that $v_z \to 0$ as $t \to t_c$.

Moreover, according to the vorticity scaling $\|\omega\|_\infty \sim (t_c - t)^{-\beta_3}$, the Beale, Kato, and Majda (BKM) [43] criterion diverges at least as $1/(t_c - t)^{\beta_3 - 1}$ as $t \to t_c$. In view of the fact that the numerical singularity of Luo and Hou [25] is spatially isotropic, these results cannot be used for the purpose of comparison. Nevertheless, the results of the simulations indicate that $\beta_3 \approx 3.46$ by employing the BKM criterion, and $\beta_3 \approx 2.91$ for the scaling for the radial component. Both estimations are greater than $3/2$, as expected.

On the other hand, it is easy to see that the resulting blow-up solution has a finite energy (8). For $\beta_3 > 3/2$, the kinetic energy coming from v_z^2 does not contribute, therefore the convergence only concerns

$$v_r^2 + v_\phi^2 = q(J^2 + w^2) \equiv \frac{q_0}{\tau(q_0, z_0)^2 + \Delta(q_0, z_0)^2}$$

[see the conservation in Appendix A], which converges for $\tau(q_0, z_0)$ and $\Delta(q_0, z_0)$ because of the assumption of a finite-energy initial flow.

The recent numerical evidence by Luo and Hou [25], as well as the analytic contribution by Elgindi [28], place a decisive step in the search of finite-time singularities in Euler equations. Both studies regard axisymmetric flows; moreover, Elgindi imposes the extra condition of a null swirl velocity. The question on singularities for an arbitrary flow, relaxing the axisymmetric configuration, remains open. Could the singularity survive to small non-axially-symmetric perturbations? On the other hand, some recent numerical study by Kerr [22] for an initial antiparallel vortex configuration discarded the existence of a finite-time singularity. Could the manifestation of a singular flow depend on the geometry and symmetries of the flow? It seems plausible, and this question deserves a more careful study.

Another question that must be regarded in more detail concerns the differences and similarities with Elgindi's work [28]. A major difference is that Elgindi imposes a null swirl velocity, meaning that the set of functions used is not class C^∞. More importantly, the nonlocal dependence of the velocity field is approximated (the Biot-Savart integral) by a simpler nonlocality. Elgindi considers nonsmooth dependence in the angular variables (Ref. [28] uses spherical coordinates instead of cylindrical coordinates used here), such that the radial dependence is a slowly varying variable compared with the angular dependence. Although the treatment of the nonlocal terms differs in both approaches, the nonsmooth dependence in the angular variables appears to be consistent with the assumption of anisotropy discussed in the current paper. Perhaps the anisotropic assumption may be relaxed by treating the nonlocal effects as Elgindi does, as has been sketched in Sec. IV E. Contrarily, for the axisymmetric flow without swirl, Elgindi neglects the advective term, $\boldsymbol{v}\cdot\boldsymbol{\nabla}$, obtaining a closed system that exhibits a finite-time singularity for the axial vorticity ω_ϕ, while in the current paper the nonlinear hyperbolic character of the equations emerges at the origin of the appearance of a nonsmooth velocity field. Finally, the secondary singularity discussed in Sec. IV G and Appendix B seems to be of the same nature as the one found by Elgindi [28].

All of these promising results point to a possible new endeavor for numerical simulations, or theoretical analysis based on anisotropic solutions in other simpler geometries, or the solution of Euler-Leray equations for a more general anisotropic flow, as well as including viscosity for the original axisymmetric flow. We shall follow this line of research in a future publication.

ACKNOWLEDGMENTS

Part of this work was done while the author was at the Universidad Adolfo Ibanez (2009–2021). The author acknowledges P. Clavin, F. Mora, and the anonymous referees for their valuable comments, which led to significant improvements in the presentation of the current version of the paper. The author express his gratitude to R. Baquero, M. Le Berre, and Y. Pomeau for their constant interest in this work as well as for numerous discussions. This work was supported by FONDECYT under Grants No. 1181382 and 1220369.

APPENDIX A: THE SOLUTION OF (25)–(28) BY MEANS OF A DYNAMICAL SYSTEMS APPROACH

The four-dimensional dynamical system (25)–(28) is formally reduced to a two-dimensional dynamical system because of the existence of two constants of motion:

$$\frac{d}{dt}(qw) = 0,$$
$$\frac{d}{dt}(q(J^2 + w^2)) = 0.$$

Thus, by virtue of these conservation laws, one can compute explicitly

$$w(q) = \frac{q_0}{q} w_0(q_0, z_0),$$

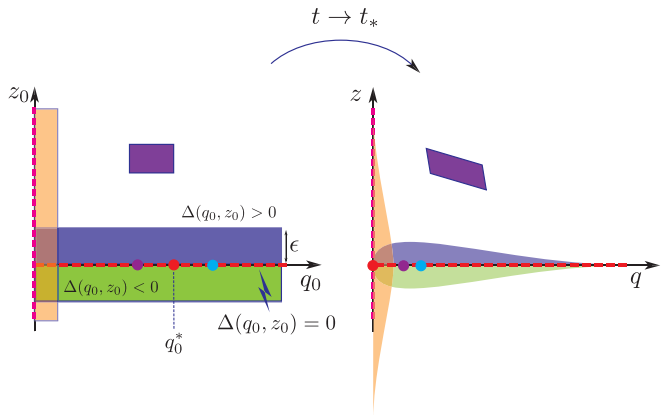

FIG. 6. Left panel: Representative regions in the q_0-z_0 plane for given initial conditions. The magenta vertical segmented line $q_0 = 0$ represents the original axis $r = 0$. The light orange zone is the neighborhood of the fixed point $q_0 = 0$. The red segmented horizontal line $z_0 = 0$ represents $\Delta(q_0, 0) = 0$ and it corresponds to $z_0 = 0$. The red point q_0^* corresponds to the minimum of $\tau(q_0, z_0 = 0)$, and we define $t_* = \tau(q_0^*, z_0^* = 0)$. The two extra points (purple, light blue) are located in the neighborhood of q_0^*. The blue and green zones belong to the neighborhood of the red segmented line $z_0 = 0$ and $\Delta(q_0, z_0) > 0$ in blue and $\Delta(q_0, z_0) < 0$ in the green region. Finally, the purple zone is an isolated region far from the q_0 and z_0 axes. Right panel: The resulting mapping representing the evolution of the initial space (q_0, z_0) into the time-dependent phase space $(q(t), z(t))$ points through the dynamical system (25)–(28). Notice that this picture is only a qualitative sketch. The only certain solutions are the orange points, and the points represented by red, light blue, and purple in the axis.

$$J^2(q) = \frac{q_0}{q}[J(q_0, z_0)^2 + w_0(q_0, z_0)^2] - \frac{q_0^2}{q^2} w_0(q_0, z_0)^2, \tag{A1}$$

where $J(q_0, z_0)$ and $w_0(q_0, z_0)$ are initial values at (q_0, z_0). By solving (25), one recovers the time-dependent evolution of $q(t)$ already calculated in Eq. (42), and the subsequent time-dependent evolution of J (40) and w (41).

However, we are interested in a more qualitative approach of the dynamical system (25)–(28), including $z(t)$. The coordinate variables $q(t)$, $z(t)$ rule the Hamiltonian dynamics (25) and (26):

$$\frac{dq}{dt} = -2\frac{\partial \psi}{\partial z}, \tag{A2}$$

$$\frac{dz}{dt} = 2\frac{\partial \psi}{\partial q} \tag{A3}$$

for a Hamiltonian $H = 2\psi$. Therefore, for a given stream function, ψ, the dynamics of $q(t)$ and $z(t)$ follows directly from Hamilton Eqs. (A2) and (A3).

Nevertheless, the evolution of (A2) and (A3) is not obvious since ψ depends formally on J according to Eqs. (19) and (A1). From a qualitative point of view, one characterizes the mapping of the dynamical system in the q-z plane (see Fig. 6).

Furthermore, the evolution of the points in phase space (q, z) is characterized by the following:

(i) The origin, $q_0 = 0$ and $z_0 = 0$, is a fixed point of the dynamics. Moreover, for any z_0 and if initially $q_0 = 0$, then $q(t) = 0$ for $t \geqslant 0$. Finally, because the q and z variables rule a Hamiltonian evolution, this is a hyperbolic point.

(ii) The surrounding region around the rotation axis $q_0 = 0$ flows according to (A2) and (A3), resulting in a deformation of the phase space around the rotation axis.

(iii) Consider the evolution of the set of points (q_0, z_0), which initially belong to the manifold $\Delta(q_0, z_0) = 0$ and $\tau(q_0, z_0) > 0$. This set of point evolves in time according to (58). The point

(q_0^*, z_0^*) reaches the origin $q \to 0$ as $t \to t_* = \tau(q_0^*, z_0^*)$, however neighboring points are excluded from the axis for $q > 0$. This behavior is at the core of the multivalued behavior in Eulerian variables J and w.

(iv) The surrounding region of the manifold $\Delta(q_0, z_0) > 0$ yields an axial velocity such that $v_\phi > 0$. The divergence-free condition implies that $v_z > 0$.

(v) The symmetric region such that $\Delta(q_0, z_0) < 0$ manifests the opposite previous flow configuration $v_\phi < 0$ (and $v_z < 0$).

(vi) Finally, the time evolution of other points preserves the area in the phase space in accordance with Hamiltonian dynamics.

The dynamical evolution of the phase space of Eqs. (25) and (26) for $0 \leqslant t < t_*$ is sketched starting with the simple initial conditions (55) and (56).

APPENDIX B: INFINITE ENERGY BLOW-UP SOLUTION

We set the particular similarity dependence in the form

$$\psi(r, z, t) = f(r^2 z, t), \tag{B1}$$

$$v_\phi(r, z, t) = r w(r^2 z, t). \tag{B2}$$

This ansatz satisfies the boundary conditions at the axis of rotation, indeed $v_r = -r\frac{\partial}{\partial \zeta} f(\zeta, t)$ with $\zeta = r^2 z$. Therefore, $\lim_{r\to 0} v_r = 0$, and, according to (B2), $\lim_{r\to 0} v_\phi = 0$. By substituting (B1) and (B2) into Eqs. (17) and (18), one obtains

$$\frac{\partial}{\partial t}\left(\frac{\partial f}{\partial \zeta}\right) = \left(\frac{\partial f}{\partial \zeta}\right)^2 - w^2, \tag{B3}$$

$$\frac{\partial w}{\partial t} = 2\left(\frac{\partial f}{\partial \zeta}\right) w. \tag{B4}$$

Therefore, the final result is a pure time-dependent ordinary differential equation for $Z(\zeta, t) = \frac{\partial}{\partial \zeta} f(\zeta, t) + i w(\zeta, t) : \frac{dZ}{dt} = Z^2$, in which the only dependence on the coordinate $\zeta = r^2 z$ comes from the initial condition

$$Z(\zeta, t) = \frac{1}{\tau(\zeta) - i\Delta(\zeta) - t},$$

which is characterized by the complex number $\tau(\zeta) - i\Delta(\zeta)$, which is directly related to the initial values for $\frac{\partial}{\partial \zeta} f(\zeta, 0)$ and $w(\zeta, 0)$.

By following the same argument as in Sec. IV G, the function shows a finite-time singularity such that if $\zeta_* \in R \quad / \quad \Delta(\zeta_*) = 0 \quad \text{and} \quad \tau(\zeta_*) = t_* > 0$, then

$$Z(\zeta_*, t) = 1/(t_* - t).$$

The above example reveals the existence of an underlying finite-time singularity. The simplified similarity dependence on the variable $\zeta = r^2 z$ brings to light the presence of a special trajectory to be understood. This trajectory is also present in the angular dependence of Elgindi's solution [28]. Essentially, it comes because the ansatz (B1) leads for the radial velocity to $v_r = -r\frac{\partial f}{\partial \zeta}$ and for the vertical velocity to $v_z = 2z\frac{\partial f}{\partial \zeta}$. Both velocities imply that, after eliminating time in (25) and (26), the characteristic equation for the axisymmetric Euler equations is

$$\frac{dr}{dz} = -\frac{r}{2z},$$

leading to $r^2 z = Cte$. Unfortunately, the ansatz (B1) and (B2) is characterized by a motion with infinite energy. Indeed, the energy

$$E = \frac{1}{2}\int \boldsymbol{v}^2\, d^3x = \pi \int_0^\infty r dr \int_{-\infty}^{\infty} \left[\left(\left(\frac{\partial f}{\partial \zeta} \right)^2 + w^2 \right) + \frac{4}{r^6}\zeta^2 \left(\frac{\partial f}{\partial \zeta} \right)^2 \right] d\zeta \to \infty$$

diverges after the radial integration. However, Elgindi finds an extra radial decaying behavior ensuring finite energy.

[1] L. Lichtenstein, Über einige existenzprobleme der hydrodynamik. Mat. Z. Phys. **23**, 89 (1925).
[2] N. Gunther, On the motion of fluid in a moving container. Izv. Akad. Nauk USSR, Ser. Fiz. Mat. **20**, 1323 (1927).
[3] J. Leray, Sur le mouvement d'un liquide visqueux emplissant l'espace, Acta Math. **63**, 193 (1934).
[4] Y. Pomeau, Singularité dans l'évolution du fluide parfait, C. R. Acad. Sci. Paris **321**, 407 (1995).
[5] Y. Pomeau, On the self-similar solution to the Euler equations for an incompressible fluid in three dimensions, C. R. Mec. **346**, 184 (2018).
[6] Y. Pomeau, M. Le Berre, and T. Lehner, A case of strong non linearity: Intermittency in highly turbulent flows, C. R. Mec. **347**, 342 (2019).
[7] Y. Pomeau and M. Le Berre, Blowing-up solutions of the axisymmetric Euler equations for an incompressible fluid, arXiv:1901.09426.
[8] D. Chae, Nonexistence of asymptotically self-similar singularities in the Euler and the Navier-Stokes equations, Math. Ann. **338**, 435 (2007).
[9] D. Chae, Nonexistence of self-similar singularities for the 3d incompressible Euler equations, Commun. Math. Phys. **273**, 203 (2007).
[10] D. Chae, On the generalized self-similar singularities for the Euler and the Navier-Stokes equations, J. Funct. Anal. **258**, 2865 (2010).
[11] H. Lamb, *Hydrodynamics* (Cambridge University Press, Cambridge, 1895).
[12] P. G. Saffman, *Vortex Dynamics*, Cambridge Monographs on Mechanics and Applied Mathematics (Cambridge University Press, Cambridge, 1995).
[13] R. Penrose, Gravitational Collapse and Space-Time Singularities, Phys. Rev. Lett. **14**, 57 (1965).
[14] D. W. Moore, The spontaneous appearance of a singularity in the shape of an evolving vortex sheet, Proc. R. Soc. London A **365**, 105 (1979).
[15] E. D. Siggia, Collapse and amplification of a vortex filament, Phys. Fluids **28**, 794 (1985).
[16] A. Pumir and E. D. Siggia, Vortex dynamics and the existence of solutions to the Navier-Stokes equations, Phys. Fluids **30**, 1606 (1987).
[17] R. H. Morf, S. A. Orszag, and U. Frisch, Spontaneous Singularity in Three-Dimensional Inviscid, Incompressible Flow, Phys. Rev. Lett. **44**, 572 (1980).
[18] M. E. Brachet, D. I. Meiron, S. A. Orszag, B. G. Nickel, R. H. Morf, and U. Frisch, Small-scale structure of the Taylor-Green vortex, J. Fluid Mech. **130**, 411 (1983).
[19] M. Brachet, M. Meneguzzi, A. Vincent, H. Politano, and P. L. Sulem, Numerical evidence of smooth self-similar dynamics for three dimensional ideal flows, Phys. Fluids A **4**, 2845 (1992).
[20] R. M. Kerr, Evidence for a singularity of the three dimensional incompressible Euler equation, Phys. Fluids A **5**, 1725 (1993).
[21] R. M. Kerr, Velocity and scaling of collapsing Euler vortices, Phys. Fluids **17**, 075103 (2005).
[22] R. M. Kerr, Bounds for Euler from vorticity moments and line divergence, J. Fluid Mech. **729**, R2 (2013).
[23] O. N. Boratav and R. B. Pelz, Direct numerical simulation of transition to turbulence from a high symmetry initial condition, Phys. Fluids **6**, 2757 (1994).
[24] J. D. Gibbon, The three-dimensional Euler equations: Where do we stand? Physica D **237**, 1894 (2008).
[25] G. Luo and T. Y. Hou, Potentially singular solutions of the 3d axisymmetric Euler equations, Proc. Natl. Acad. Sci. (USA) **111**, 12968 (2014).

[26] D. Barkley, A fluid mechanic's analysis of the teacup singularity, Proc. R. Soc. London A **476**, 20200348 (2020).
[27] T. M. Elgindi and I.-J. Jeong, Finite-time singularity formation for strong solutions to the axi-symmetric 3D Euler equations, Ann. PDE **5**, 16 (2019).
[28] T. M. Elgindi, Finite-time singularity formation for $C^{1,\alpha}$ solutions to the incompressible Euler equations on $\mathbb{R}^3$. Ann. Math. **194**, 647 (2021).
[29] M. P. Brenner, S. Hormoz, and A. Pumir, Potential singularity mechanism for the Euler equations, Phys. Rev. Fluids **1**, 084503 (2016).
[30] P. Constantin, P. D. Lax, and A. Majda, A simple one-dimensional model for the three-dimensional vorticity equation, Commun. Pure Appl. Math. **38**, 715 (1985).
[31] S. De Gregorio, On a one-dimensional model for the three-dimensional vorticity equation, J. Stat. Phys. **59**, 1251 (1990).
[32] S. De Gregorio, A partial differential equation arising in a 1D model for the 3D vorticity equation, Math. Methods Appl. Sci. **19**, 1233 (1996).
[33] C. Josserand, Y. Pomeau, and S. Rica, Finite-time localized singularities as a mechanism for turbulent dissipation, Phys. Rev. Fluids **5**, 054607 (2020).
[34] L. D. Landau and E. M. Lifshitz, *Fluid Mechanics* (Pergamon, New York, 1959).
[35] A. J. Majda and A. L. Bertozzi, *Vorticity and Incompressible Flow*, Cambridge Texts in Applied Mathematics (Cambridge University Press, Cambridge, 2001).
[36] J. D. Gibbon, D. R. Moore, and J. T. Stuart, Exact, infinite energy, blow-up solutions of the three-dimensional Euler equations, Nonlinearity **16**, 1823 (2003).
[37] J. Nečas, M. Růžička, and V. Šverák, On Leray's self-similar solutions of the Navier-Stokes equations, Acta Math. **176**, 283 (1996).
[38] E. Kasner, Geometrical theorems on Einstein's cosmological equations, Am. J. Math. **43**, 217 (1921).
[39] R. Grauer and T. C. Sideris, Numerical Computation of 3D Incompressible Ideal Fluids with Swirl, Phys. Rev. Lett. **67**, 3511 (1991).
[40] A. Pumir and E. D. Siggia, Finite-Time Singularities in the Axisymmetric Three-Dimension Euler Equations, Phys. Rev. Lett. **68**, 1511 (1992).
[41] T. Tao, Elgindi's approximation of the Biot-Savart law, https://terrytao.wordpress.com/tag/tarek-elgindi/.
[42] M. R. Ukhovskii and V. I. Iudovich, Axially symmetric flows of ideal and viscous fluids filling the whole space, J. Appl. Math. Mech. **32**, 52 (1968).
[43] J. T. Beale, T. Kato, and A. Majda, Remarks on the breakdown of smooth solutions for the 3-d Euler equations, Commun. Math. Phys. **94**, 61 (1984).